Applied Surface Science 285P (2013) 469–476

Contents lists available at ScienceDirect

Applied Surface Science

journal homepage: www.elsevier.com/locate/apsusc

Effect of film compatibility on electro-optic properties of dye doped polymer DR1/SU-8

Xiaoqiang Sun[a,b], Ying Xie[a], Xuliang Zhao[a], Dehui Li[a], Shimin Zhao[a], Yuanbin Yue[a], Xibin Wang[a], Jian Sun[a], Lei Liang[a], Changming Chen[a], Daming Zhang[a], Fei Wang[a,*], Zhiyuan Xie[b]

[a] State Key Laboratory on Integrated Optoelectronics, Jilin University, No. 2699, Qianjin Street, Changchun, Jilin 130012, China
[b] Changchun Institute of Applied Chemistry, Chinese Academy of Sciences, No. 5625, Renming Street, Changchun, Jilin 130022, China

ARTICLE INFO

Article history:
Received 28 March 2013
Received in revised form 15 August 2013
Accepted 19 August 2013
Available online 27 August 2013

Keywords:
Electro-optic polymers
Compatibility
Passive cladding
Waveguide

ABSTRACT

The physic-chemical compatibility of passive cladding and poled Dispersed Red 1 (DR1) doped ultraviolet (UV) curable polymer SU-8 was investigated. The multilayer films consisting of DR1/SU-8 core and Norland Optical Adhensive 73 (NOA73), SU-8, polydimethylsiloxane (PDMS), or polymethylmethacrylate (PMMA) upper-cladding were fabricated on the silicon substrate, respectively. The interface morphologies were characterized through scan electronic microscope. Parallel plate electric field poling was carried out to align the polarity of chromophores in SU-8. The core–cladding interface with no chemical erosion or delamination was obtained by adopting an excess UV exposure and higher temperature dealing when NOA73 was used as the upper-cladding. The root mean square roughness of the upper-cladding surface was measured by atomic force microscope to verify the poling process. The electro-optic (EO) signal response amplitude of these multilayer films was used to characterize the polarizability alignment of DR1 chromophores by means of Teng–Man method after poling. Resistivity of claddings was measured at the glass transition temperature of DR1/SU-8 to explain the EO response difference. The configuration of NOA73/(DR1/SU-8) exhibited the best EO performance and time relaxation in amplitude within 550 h by prolonging the cooling time in poling process. A channel waveguide was fabricated to study the poling-induced optical loss. The results show that the selection of passive cladding with favorable electrical and chemical property is essential to establish optical nonlinearity in the dye–polymer system.

1. Introduction

Electro-optic (EO) polymers are prospective materials with many favorable merits for various applications, including optical network components, on-chip optical interconnects [1–3], microwave photonics and others [4–6]. They have specialties of large EO coefficients, low optical loss at 1.30 and 1.55 μm telecommunication wavelengths, low dispersion of refractive index (RI) between optical frequencies and millimeter waves, easy to process and relatively low cost. Nonlinear polymers and chromophores with high molecular polarizability have been designed, tailored and introduced from molecular engineering both theoretically and synthetically [7–9]. However, most of these materials are not commercially available yet. Consequently, these excellent outcomes of molecular engineering are incapable of playing desirable roles for the worldwide development of organic EO devices. Among nonlinear optical systems, guest–host polymers need no chemical attachment of chromophores to the host polymer and can be synthesized at a lower cost than any other systems, including side-chain, cross-linked, and main-chain polymers that are synthesized with more complicated reaction [10–12]. Recently, we have demonstrated the approach to overcome disadvantages of guest–host system that fast decay of nonlinear property and low chromophores concentration by using a high glass transition temperature (T_g) host polymer SU-8 doped with organic chromophores Dispersed Red 1 (DR1) that has good miscibility with SU-8 [13].

Practical optical waveguide devices require the active layer to be sandwiched between two cladding layers [14]. For EO waveguide, compatible buffer and cladding layers are necessary for light guiding in the active core. These claddings commonly have characteristics of similar thickness with the active layer, relatively low optical loss, and appropriate RI supporting mode propagation [15]. Another essential request for the sandwiched layers is to build an effective poling field through the multilayer geometry to achieve

* Corresponding author. Tel.: +86 0431 851 680 97; fax: +86 0431 851 680 97.
E-mail address: wang_fei@jlu.edu.cn (F. Wang).

0169-4332/$ – see front matter © 2013 Elsevier B.V. All rights reserved.
http://dx.doi.org/10.1016/j.apsusc.2013.08.079

a quasi-permanent alignment of polarizability of chromophores [16]. Previous studies have shown that effective poling is highly dependent upon factors of voltage division between the multiple-layers, chemical and optical characteristics of individual layers with respect to temperature, and chromophore–chromophore interaction [17,18]. Thus, favorable core–cladding physic-chemical compatibility is crucial for polymer EO waveguide fabrication.

In this paper, we report on the investigation of physic-chemical compatibility of poled dye doped polymer and passive claddings of Norland Optical Adhensive 73 (NOA73), SU-8, polydimethylsiloxane (PDMS) and polymethylmethacrylate (PMMA). We present experimental results on the interface morphology through scan electronic microscope (SEM) and effects of electric field poling on cladding surface roughness by atomic force microscope (AFM). According to the measurement of EO signal amplitude and time stability, NOA73 as upper-cladding is more preferable to obtain stable optical nonlinearity and minimal poling-induced optical loss.

2. Experiment

2.1. EO polymer preparation

To synthesize the EO material, 5 wt% DR1 was doped into the widely used polymer SU-8 2005 (MicroChem Corp.) and thoroughly stirred to ensure complete mixing. Ultraviolet (UV) curable SU-8 can realize chemical cross-linking because high absorption of DR1 exists in the UV region and photoacid presents neutralization because of the chromophores [13]. To enhance the above process and reduce chromophores relaxation, 3.5 wt% triarylsulfonium salt photoinitiator was introduced into the EO polymer of DR1/SU-8.

2.2. Multilayer sample fabrication

Firstly, the ground electrode of 500 nm aluminum was thermally evaporated onto the backside of a conductive silicon substrate with a low resistivity of 0.002 Ω cm. A 5 μm thick DR1/SU-8 film was formed by spin-coated process on the front side. The sample was pre-baked at 65 °C for 10 min and 90 °C for 20 min to remove the residual solvent. Then, it was UV cured by a mercury (Newport Co., 10 mW/cm^2 at 365 nm) lamp for 180 s, followed by a post-exposure baking at 95 °C for 15 min and 135 °C for 1 h to enhance the cross-linking of EO polymer. Commercialized polymers of PMMA (Sigma Aldrich Inc.), NOA73 (Norland Products Inc.), PDMS (Dow Corning Corp.) and SU-8 were spin-coated onto the DR1/SU-8 film as the passive upper-cladding and cured under different conditions, respectively. PMMA solution was spin-coated at 3000 rpm and baked at 120 °C for 150 min, yielding a 4 μm thick film. A solvent-free UV curable polymer NOA73 was spin-coated at 4000 rpm, yielding a 4.5 μm thick film. Then, it was exposed under the mercury lamp for 170 s and post-exposure baked at 110 °C for 100 min to enhance cross-linking. Thermal cured PDMS solution was spin-coated at 2000 rpm and yielding a 2.5 μm thick film. Then, it was cured at 85 °C for 3 h to remove the residual solvent. The pure SU-8 thin film cladding was deposited according to the same cross-linkable process as that of DR1/SU-8.

2.3. Electric field poling

Parallel plate electric field poling was used to preferentially align DR1 chromophores and induce a nonzero EO coefficient γ_{33}. The schematic view of experimental setup is shown in Fig. 1. To be practically useful, the poling field was supposed to be as large as possible and chosen to be weaker than the dielectric breakdown voltage of polymers. The substrate temperature was controlled by a lab-made heater and the temperature controller. Firstly, a field of 100 V/μm was applied to the prepared sample in 25 V steps every 0.1 min at room temperature. After the full field was applied, the temperature was raised to T_g (200 °C) of DR1/SU-8 at a rate of 15 °C/min to avoid decomposition of chromophores [19,20]. The poling field was kept for 30 min at the optimum poling temperature. Once the poling time was reached, the sample was slowly cooled to room temperature to allow the voltage removed without loss of chromophores alignment by chilled water coils incorporated into the hotplate [21].

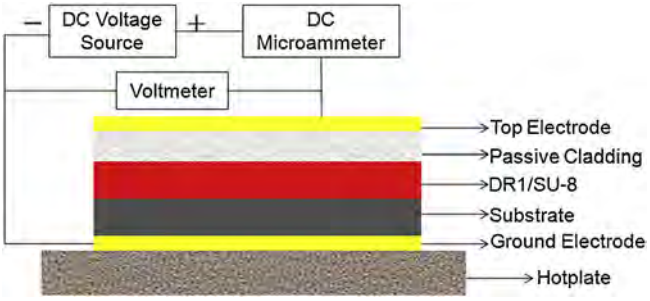

Fig. 1. Schematic view of experimental setup for parallel plate electric field poling.

2.4. Waveguide fabrication

A straight channel waveguide was used to study the optical loss. Fig. 2 presents the schematic diagram of fabrication process. Firstly, DR1/SU-8 was spin-coated onto a 3 μm thick silica lower cladding on silicon substrate. After the same material process introduced in Section 2.2, a layer of 100 nm thick aluminum film was thermal evaporated onto the top of DR1/SU-8 film as the metal mask. To define waveguide patterns on aluminum film, BP212 photoresist was spin-coated and patterned by traditional photolithography (ABM Co. Inc., USA) [22]. The oxygen inductively coupled plasma etching process was performed for 150 s in a 13.56 MHz CE-300I (ULVAC Co. Inc., Japan) etching machine [23,24]. Before the optical loss measurement, the waveguide sample was sliced by a wafer dicing machine DAD-3220 (DISCO Co. Inc., Japan) to minimize the uncertainty of input/output coupling loss.

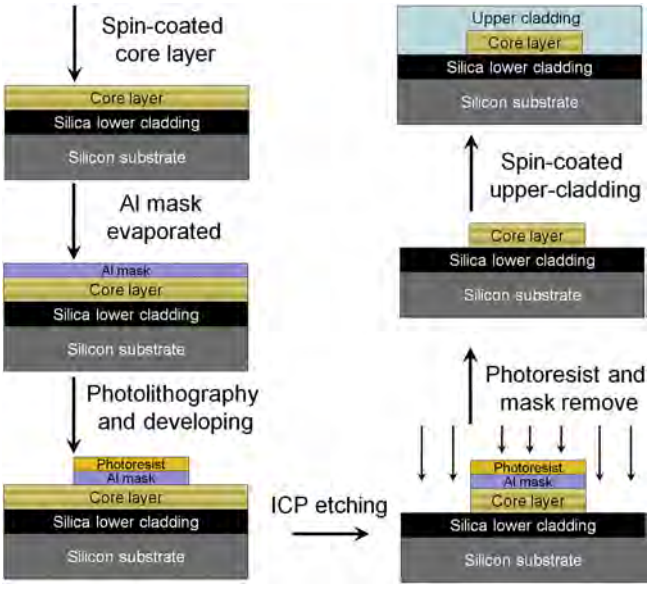

Fig. 2. Schematic diagram of DR1/SU-8 channel waveguide fabrication process.

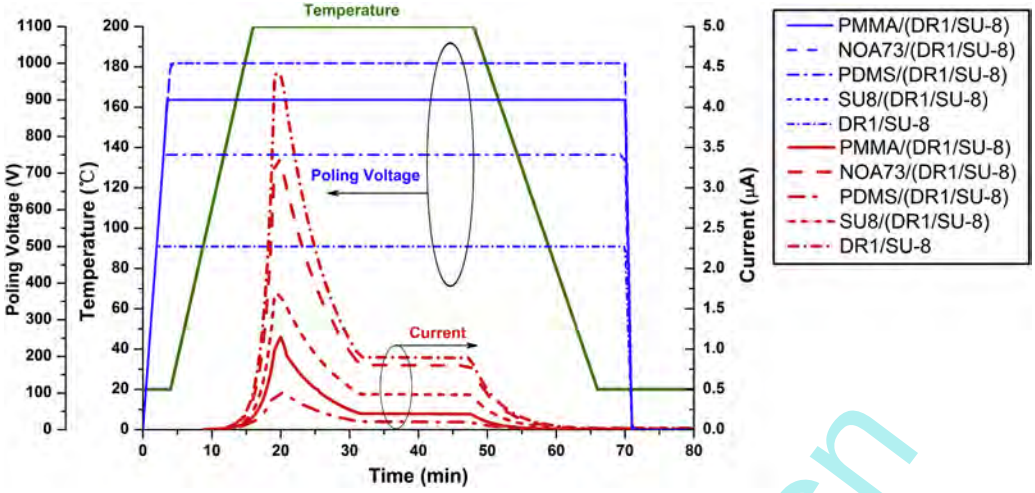

Fig. 3. Temperature, voltage, and current profile of parallel-plate poling for polymer films.

2.5. Characterization

Refractive indices of DR1/SU-8, NOA73, PDMS, SU-8 and PMMA measured by spectroscopic ellipsometry M-2000UI (J. A. Woollam Inc., USA) at 1550 nm were 1.57, 1.55, 1.41, 1.56 and 1.48, respectively. The characterization of cross-section view of multilayer films was examined by means of SEM machine JSM-7600F (JEOL Ltd., Japan) that operated on voltage of 5 kV. After the top electrode was removed from the poled films, AFM images were recorded with a multimode scanning probe microscope CSPM5000 (Being Nano-Instrument Ltd., China) that operated in contact mode to measure the root mean square (RMS) roughness of the upper-cladding surface [25,26]. The EO signal amplitude of poled films was measured by Teng–Man setup. The output from a tunable semiconductor laser operating at 1550 nm was butt-coupled through a standard single mode fiber (SMF) into the straight channel waveguide fabricated in Section 2.4. The poling-induced optical loss of a 4 μm wide waveguide was measured by cutback method.

3. Results and discussion

3.1. Poling voltage and current

When parallel plate poling is conducted, the poling voltage is chosen to be 500, 750, 900, and 1000 V with respect to the film thickness of multilayer films, supposing the electric fields in all films are the same. The temperature, voltage and current profile are measured and illustrated in Fig. 3. Because of the resistivity

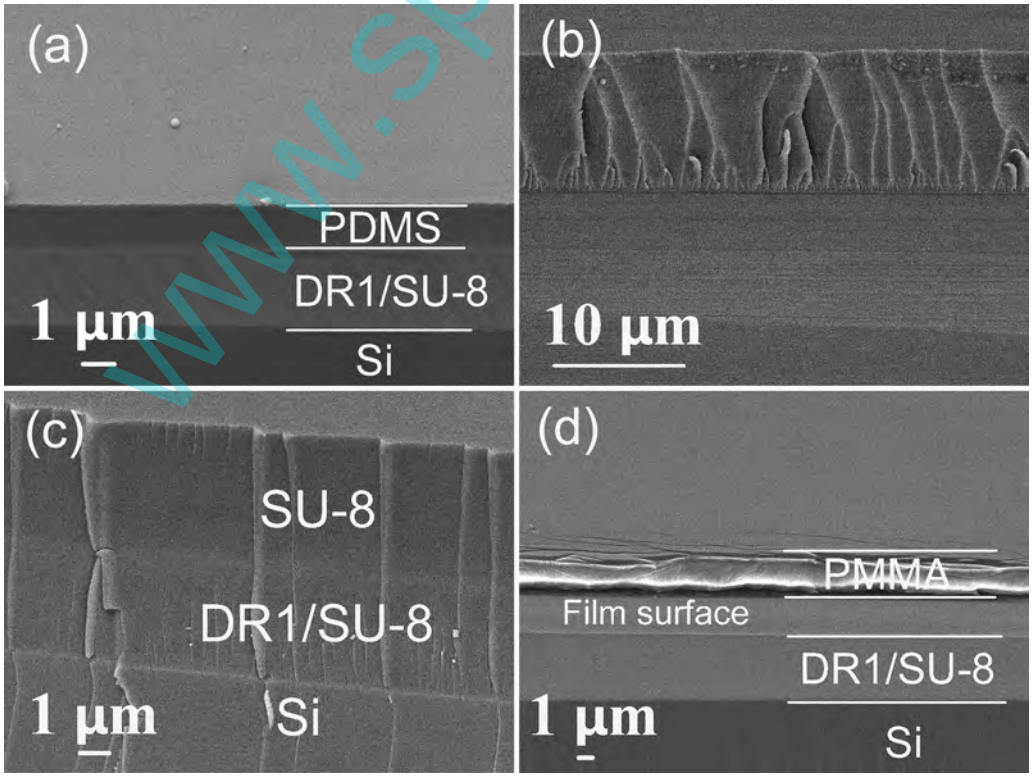

Fig. 4. Cross-section SEM images of multilayer interface. (a) PDMS, (b) NOA73, (c) SU-8, and (d) PMMA above DR1/SU-8 film.

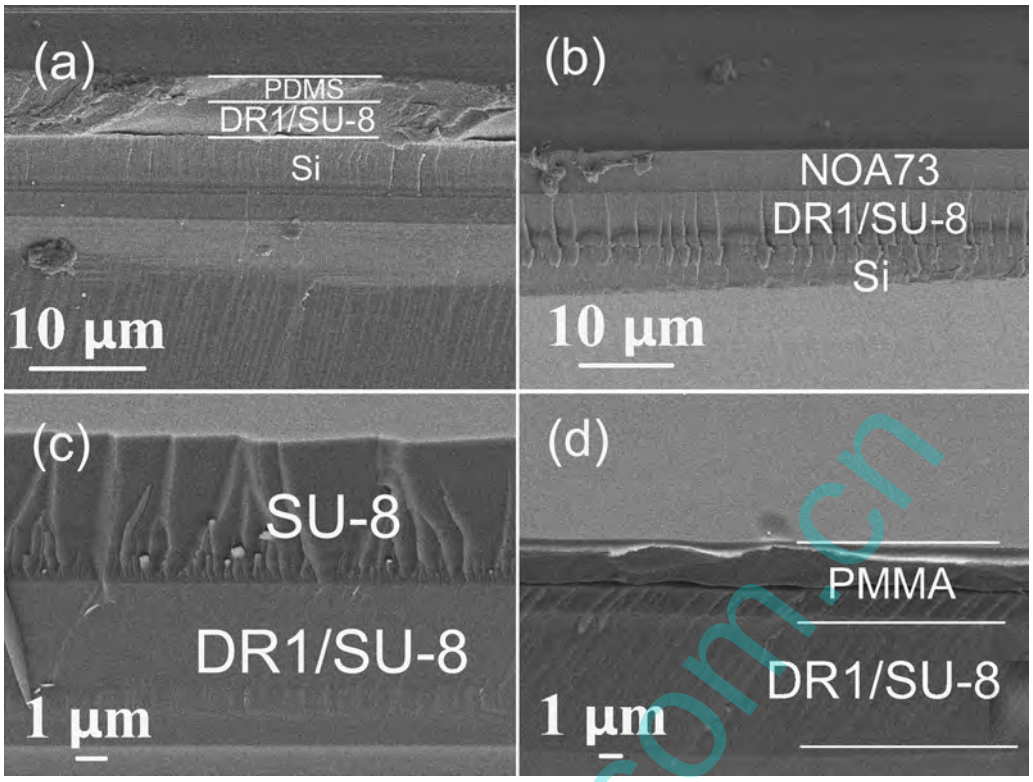

Fig. 5. Cross-section SEM images of multilayer interface after 30 s UV exposure and 135 °C baking for 1 h. (a) PDMS, (b) NOA73, (c) SU-8, and (d) PMMA above DR1/SU-8 film.

difference of claddings, the currents present diverse amplitude change. As shown in the figure, the current rises quickly with the decline of polymer resistance which is due to the temperature increasing. A maximum of current appears after about 10 min once the temperature reached 200 °C. With the progress of poling, the disordered chromophores gradually align with the direction of poling field, resulting in an inner electric field reversed with the direction of outside poling field that leads to the decrement of current. It should be noted the current falls rapidly after the peak appears, which indicates that the rotation of DR1 chromophores is relatively easy. However, this movement gets harder with the establishment of inner electric field induced by the alignment of chromophores. After 30 min poling, the current becomes stable, implying the accomplishment of poling. When multilayer films cool to room temperature, the current almost falls to zero due to the repristination of polymer resistivity.

3.2. Interface between layers

The physic-chemical compatibility of core–cladding couples has remarkable influence on the waveguide fabrication techniques and EO performance. Hence, the interface morphology between DR1/SU-8 film and passive cladding is investigated. Fig. 4 shows SEM images of the cross-section view of multilayer films fabricated in Section 2.2. A clear interface can be observed in Fig. 4(a) when PDMS was spin-coated. It proves that DR1/SU-8 film is solid enough to stand the erosion of cycloheptane solvent in PDMS due to its cross-linking process. No clear interface is observed in Fig. 4(b) because of some reason. However, the whole thickness of 10 μm equals the sum of NOA73 and DR1/SU-8 film. Thus, we can suppose that this indistinct interface was owing to the close RI of these two materials. Blurred borderline is observed in Fig. 4(c), which implies that inconspicuous dissolution has happened at the interface. This reaction damages the chemical property of DR1/SU-8, especially the orientation stability of chromophores that determines the optical nonlinearity. An obvious delamination can be observed in Fig. 4(d), which means PMMA cladding does not possess good adhesion on DR1/SU-8 film. This results in the shrinkage and exposure of underlayer, which is unfavorable for waveguide cladding application.

To strengthen the physic-chemical stability of multilayer films, a further 30 s UV exposure and 135 °C higher temperature heat dealing was adopted to enhance the cross-linking of SU-8. Cross-section SEM images of interfaces are shown in Fig. 5, the cladding contrasts evidently with DR1/SU-8 film. However, an unclear interface appears in Fig. 5(a), which may result from the slicing. Compared with that in Fig. 5(c), a clearer borderline can be seen in Fig. 5(c), which is owing to the further cross-linking of SU-8. A gap emerges in PMMA cladding, as shown in Fig. 5(d). It indicates that some chemical reaction has happened at the interface, which leads to part of the PMMA cladding peeled off. This is completely unacceptable for EO waveguide application. Fortunately, a perfect interface appears between NOA73 and DR1/SU-8 layer, as shown in Fig. 5(b). To explain this difference, more detailed studies about NOA73 were carried out. It is found that the viscosity of NOA73 is moderate to be 140 cps at 25 °C that facilitates direct deposition on EO film by spin-coated process. Besides, it does not contain any organic solvent, which avoids possible chemical reaction between dye-doped polymer and this upper-cladding that would otherwise erode the EO layer.

3.3. Poling effects

The samples were also characterized after poling process introduced in Section 2.3. Cross-section SEM images of the interface are shown in Fig. 6. Compared with state before poling, the interface in Fig. 6(c) is clearer. However, SU-8 cladding becomes fragile and the tenacity decreased, too. This indicates that the physic-chemical property has changed during the high temperature poling process. The adhesion problem of PMMA still exists after poling, as

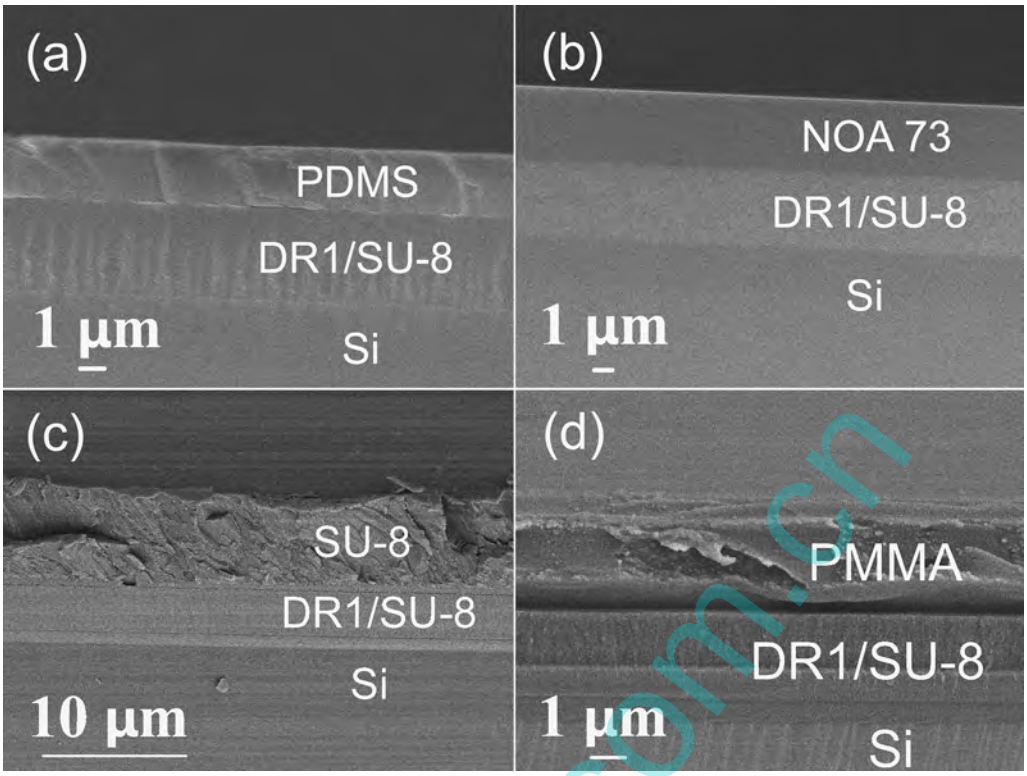

Fig. 6. Cross-section SEM images of multilayer interface after poling. (a) PDMS, (b) NOA73, (c) SU-8, and (d) PMMA above DR1/SU-8 film.

shown in Fig. 6(d). An obvious crack can be seen in this case. These unfavorable features destroy the promise of SU-8 and PMMA as upper-cladding in waveguide configuration. Contrastingly, a clear interface and flat cross-section can be obtained when NOA73 or PDMS was spin-coated on DR1/SU-8, as shown in Fig. 6(a) and (b). It indicates that no certain evidence of chemical erosion or thermal expansion induced film shrinkage has happened, which is favorable for the alignment of chromophores and reduction of optical loss.

It has been reported that RMS roughness can characterize the alignment of chromophores with the poling direction [27,28]. Thus, the cladding surface is measured by AFM before and after poling, as shown in Figs. 7 and 8. For all these multilayer films, the measurement is performed on several samples, and the error is weighted accordingly. The measurement results show that no RMS roughness is larger than 3 nm, and all cladding surfaces are clean and flat before poling. However, the surface quality changes and RMS roughness increases after poling. It predicates that DR1 choromophores have rotated along the poling electric field direction. Moreover, the RMS roughness of cladding surface is different from each other. This may result from the inner stress that formed inside the multilayer films during poling, which includes the increment and decrease of temperature [29]. Furthermore, according

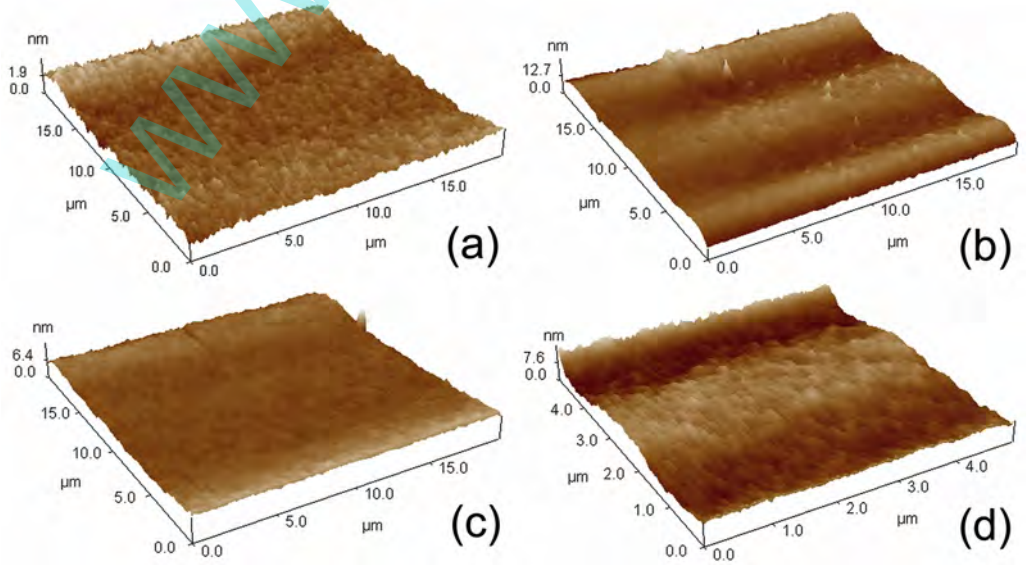

Fig. 7. AFM images of cladding surface before poling, the RMS roughness is (a) PDMS: 0.336 nm, (b) NOA73: 2.84 nm, (c) SU-8: 0.767 nm, and (d) PMMA: 2.17 nm, respectively.

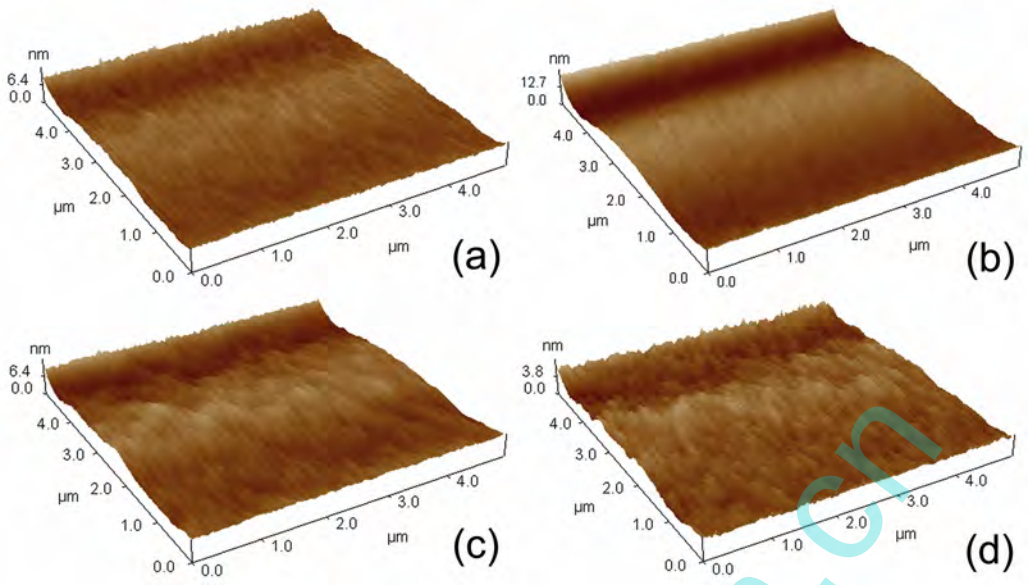

Fig. 8. AFM images of cladding surface after poling, the RMS roughness is (a) PDMS: 22.3 nm, (b) NOA73: 18.4 nm, (c) SU-8: 9.55 nm, and (d) PMMA: 14 nm, respectively.

to our previous work, this increased roughness may induce excess optical loss that will be discussed in Section 3.4. Thus, a smoother cladding surface is more preferable for low loss EO waveguide.

3.4. EO characteristic difference

To confirm the EO characteristic of poled polymer, the EO signal amplitudes of DR1/SU-8 film with the above claddings are measured by means of Teng–Man technique at 1 kHz frequency of modulation electric field [30]. For the dual layer films with both a polymer core and cladding layer, a corrected Teng–Man expression was used to calculate EO coefficient [31]. Here, we just use the response amplitude to characterize the optical nonlinearity of polymer film. As shown in Table 1, when NOA73 is chosen as the cladding, the EO signal amplitude is very close to that of the single DR1/SU-8 film. When SU-8 or PDMS is adopted as upper-cladding, the EO signal amplitude is much smaller than that of NOA73.

This can be explained by the resistivity characteristic of polymers that EO core should possess a significantly higher resistance than that of claddings over the entire range of temperature experienced in poling, from room temperature to T_g. The resistivity of NOA73 or SU-8 at a certain temperature has been reported [32]. However, data quoted in the literature for a given material usually spans several orders of magnitude, depending on factors of sample preparation, degree of polymerization, layer quality, purity, and others. Thus, the resistivity of polymers used in this study was measured at the poling temperature of 200 °C. To perform this measurement, the single polymer film is deposited between two golden electrodes as in the case of poling. The sample is placed in the center of a thermostatic container. The applied voltage and electric current between electrodes are ensured by a high resistance meter (Dongwen, P503, China). According to Eq. (1)

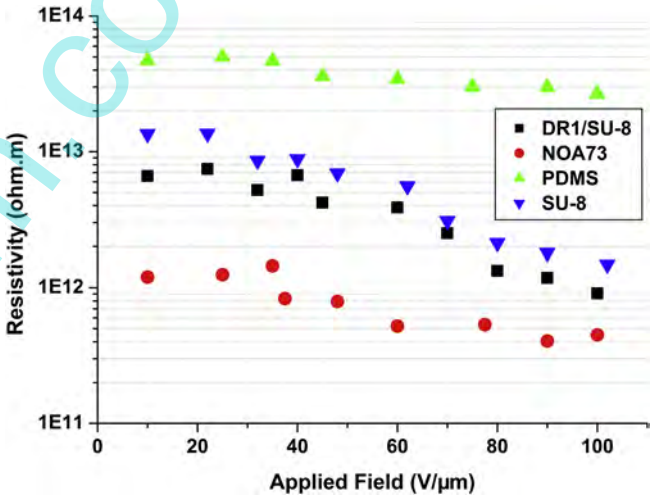

Fig. 9. Resistivity of polymers as a function of the applied voltage at 200 °C.

$$\rho = \frac{V}{I}\frac{S}{t} \tag{1}$$

where V is the potential drop across the polymer layer, S is the area of the polymer perpendicular to the potential gradient, I is the current between electrodes, and t is the current path length, resistivity of cladding and DR1/SU-8 polymer as a function of the applied voltage can be calculated. The measurement results are shown in Fig. 9. The dual layer films of NOA73/(DR1/SU-8) is expected to display a stronger EO response after parallel plate poling than others because

Table 1
EO signal amplitude of dual layer films cladding/(DR1/SU-8) before and after poling parameter optimization (prolonging the cooling time).

Multilayer film	DR1/SU-8	PDMS/(DR1/SU-8)	NOA73/(DR1/SU-8)	SU-8/(DR1/SU-8)
Poling parameter before optimization (mV)	240	42	166	95
Poling parameter after optimization (mV)	548	127	358	233

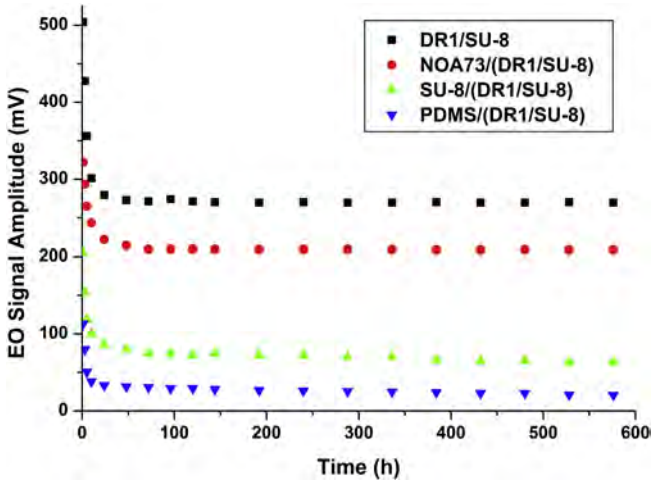

Fig. 10. Time relaxation of the EO signal amplitude of multilayer films after poling.

the resistivity NOA73 ($3.5 \times 10^{11}\ \Omega$ cm) is only a quarter of SU-8, or a third of DR1/SU-8 ($9.5 \times 10^{11}\ \Omega$ cm). When NOA73 is used as the cladding material, this low resistivity would allow 72% of the applied voltage to be dropped across the DR1/SU-8 layer, resulting in high poling field [33]. When PDMS is used as the cladding, the EO response amplitude is much lower than that of others because the relatively high resistivity $8.6 \times 10^{12}\ \Omega$ cm of PDMS is nearly one order of magnitude larger than that of DR1/SU-8. Though the film thickness of PDMS is just one half of that of NOA73, only 17% of the applied voltage would drop across the DR1/SU-8 layer.

For practical waveguide application, the EO response time stability in multilayer films needs to be confirmed, too. It has been reported that the thermal stability of the second order optical nonlinearity of a poled dye-doped polymer can be improved when the physical aging temperature coincides with the decay temperature. Thus, we prolong the aging time to 2 h to decrease the free volume of the polymer matrix and make it more compact around the oriented dopants to hinder the rotation of chromophores out of the alignment [34,35]. The EO signal amplitude after poling parameters optimized is shown in Table 1. Compared with normal process, all EO signal amplitude enlarges over two times, which proves the effectiveness of physical aging to enhance EO response of this dye-doped UV polymer. The time relaxation of EO signal amplitude was measured periodically to verify the alignment stability [36]. As shown in Fig. 10, all EO responses show magnitude degradation with time, and become stable after 100 h. Moreover, NOA73/(DR1/SU-8) system exhibits the best optical nonlinearity and time stability amongst these multilayer films.

Since the interaction mechanism between azo dye and host molecules is different from side chain or main chain EO polymers [37], the time stability comparison is just carried out between DR1/SU-8 and other DR1 doped guest–host polymers, including DR1/poly(bisphenol A carbonate)(PC), DR1/PMMA, DR1/sol–gel and DR1/poly(2-vinylpyridine)(P2VP). Like other characterization parameters, such as order parameter, EO coefficient γ_{33} and nonlinear optical coefficient d_{33} that have been adopted to characterize optical nonlinearity, EO signal amplitude can be used to prove the stability performance of DR1/SU-8 multilayer films. Normalized order parameters of DR1/PC, DR1/PMMA are measured at room temperature over a period of 24 days in Ref. [38]. They decrease to stabilized values after about 10 days. After stabilization, the order parameter for DR1/PC retains 86% of its original value, while for DR1/PMMA it decays to 69%. Another relaxation measurement of γ_{33} for 10% doped DR1/P2VP demonstrates that the EO coefficient only retains 50% of its original value after 4 days [39]. For DR1 doped sol–gel material, the d value was stable for up to 80 days at room temperature without initial or long term relaxation [40]. Several factors determine the initial order parameter and the orientation retention of DR1 molecules, including poling electric field and temperature, hydrogen bonding of the hydroxyl group of DR1 to carbonyl groups of host polymer, and cladding resistivity. The EO signal amplitude of DR1/SU-8 reduces 45%, and NOA73/(DR1/SU-8) films reduces 37% from their original values after 10 days. Though the stability performance of NOA73/(DR1/SU-8) films is not the best, they remained essentially constants for the application in EO waveguide devices.

Table 2
Optical loss of the channel waveguide before and after poling.

Claddings	Before poling (dB/cm)	After poling (dB/cm)	Poling-induced loss (dB/cm)
NOA73	2.6	3.9	1.3
PDMS	1.7	3.8	2.1
SU-8	2.8	4.2	1.4

3.5. Optical loss

The determination of optical loss lies in the measurement of transmitted power according to the waveguide length [41]. A straight channel waveguide was fabricated to study the optical loss introduced in Section 2.4. The optical loss before and after poling per unit length, measured by cleaving back the waveguide in steps of 5 mm is shown in Table 2 [42]. The uncertainty of the measurement is convinced to be <0.5 dB/cm because of the repeatability of chip cleaving [43]. As shown in Table 2, the waveguide adopting PDMS as upper-cladding has the smallest optical loss of 1.7 dB/cm before poling. The waveguide adopting NOA73 or SU-8 as upper-cladding exhibits a larger optical loss. Since the upper-cladding RI increment of from 1.41 to 1.56 is consistent with the sequence of optical loss change, we can reasonably reckon that the optical loss has close relationship with the RI contrast between the core and cladding material, which confines the mode field in waveguide. The higher the RI contrast is, the more optical power is confined in the core layer.

After poling, the surface of poled area is exposed by removing the top electrode. Except for RMS roughness increment revealed in Section 3.3, inhomogeneities regions of several micrometers can be observed under contrast-enhanced microscope because of the existence of weak dielectric spots in the cladding layer that affects the local poling field. Therefore, the optical loss of samples increases apparently with the appearance of inhomogeneities in the media that are amplified during poling process. Besides, the magnitude of poling-induced loss is not strictly in accordance to that of the RI sequence. This can be explained by the difference of cladding dielectric property and interface morphology between core–cladding couples after poling. Though the waveguide with PDMS as upper-cladding presents the lowest optical loss of 3.8 dB/cm after poling, the waveguide adopting NOA73 as upper-cladding shows a lowest poling-induced optical loss of about 1.3 dB/cm, which leads to a compromise optical loss of 3.9 dB/cm after poling.

4. Conclusion

In this study, physic-chemical compatibility of passive cladding and guest–host EO polymer DR1/SU-8 was investigated. SEM images of multilayer films interface morphologies demonstrated that excess UV exposure and high temperature dealing can enhance the cross-linking and solidity of DR1/SU-8, preventing it from chemical erosion and delamination. The measured EO signal amplitude and RMS roughness change of the multilayer films surface

proved the alignment of DR1 molecules in SU-8 by means of Teng–Man method after parallel plate poling. Resistivity of polymer claddings indicated the origin of EO response distinction of core–cladding couples. The optical nonlinearity and time stability can be improved by prolonging cooling time in poling process. As a result, NOA73 as cladding suggests the low optical loss, strong and stable EO response for DR1/SU-8 waveguide, compared with PDMS, SU-8 or PMMA polymers. This series of characterizations in this paper can be used to find passive claddings with favorable electrical and chemical property for EO polymer waveguide application.

Acknowledgements

This work is supported by the National Natural Science Foundation of China (Nos. 61177027, 61107019, 61077041, 61205032), Science and Technology Development Plan of Jilin Province (No. 20110315), Program for Special Funds of Basic Science & Technology of Jilin University (Nos. 201100253, 201103071), China Postdoctoral Science Foundation (Nos. 2011M500597, 2012M510900).

References

[1] Y. Enami, C.T. Derose, D. Mathine, C. Loychik, C. Greenlee, R.A. Norwood, T.D. Kim, J. Luo, Y. Tian, A.K.-Y. Jen, N. Peyghambarian, Hybrid polymer/sol–gel waveguide modulators with exceptionally large electro-optic coefficients, Nature Photonics 1 (2007) 180–185.
[2] D.L.K. Eng, S. Kozacik, B.C. Olbricht, S. Shi, D.W. Prather, Broadband low-drive voltage polymer electro-optic modulator, Proceedings of SPIE 8259 (2012) 82590C.
[3] R. Rita Asquini, A. d'Alessandro, A. Salusti, C. Gizzi, Design of a wideband tunable AWG using electro-optic polymers and push–pull electrode configuration for ultrafast photonic switching applications, Proceedings of SPIE 5246 (2003) 323–332.
[4] W.C. Wang, R. Forber, K. Bui, Compact super wideband optical antenna, Proceedings of SPIE 7316 (2009) 731614.
[5] C.-Y. Lin, A.X. Wang, X. Zhang, B.S. Lee, R.T. Chen, EO-polymer waveguide based high dynamic range EM wave sensors, Proceedings of SPIE 8258 (2012) 82580Y.
[6] L.R. Dalton, D. Lao, B.C. Olbricht, S. Benight, D.H. Bale, J.A. Davies, T. Ewy, S.R. Hammond, P.A. Sullivan, Theory-inspired development of new nonlinear optical materials and their integration into silicon photonic circuits and devices, Optical Materials 32 (2010) 658–668.
[7] L.R. Dalton, Theory-guided design of organic electro-optic materials and devices, Polymers 3 (2011) 1325–1351.
[8] L.R. Dalton, P.A. Sullivan, D.H. Bale, Electric field poled organic electro-optic materials: state of the art and future prospects, Chemical Reviews 110 (2010) 22–55.
[9] L.R. Dalton, Theory-inspired development of organic electro-optic materials, Thin Solid Films 518 (2009) 428–431.
[10] S.-H. Jang, A.K.-Y. Jen, Polymeric second-order nonlinear optical materials and devices, in: S.-S. Sun, L.R. Dalton (Eds.), Introduction to Organic Electronic and Optoelectronic Materials and Devices, CRC Press, New York, 2008, pp. 467–512.
[11] P.A. Sullivan, B.C. Olbricht, L.R. Dalton, Advances in organic materials for optical modulation, Journal of Lightwave Technology 26 (2008) 2345–2354.
[12] S.-L. Liu, H. Ang, R.-l. Jin, Z.-x. Yan, M.-b. Yi, Electro-optic properties of DR1 doped SiO_2 organic/inorganic guest–host films, Chemical Research in Chinese Universities 25 (2009) 726–732.
[13] C.M. Chen, X.Q. Sun, D. Zhang, Z.B. Shan, S.-Y. Shin, D.M. Zhang, Dye-doped polymeric planar waveguide devices based on a thermal UV-bleaching technique, Optics & Laser Technology 41 (2009) 495–498.
[14] H. Zhang, D.H. Chang, C. Zhang, C. Wang, W.H. Steier, H.R. Fetterman, Electrooptic polymer modulators with an inverted-rib waveguide structure, IEEE Photonics Technology Letters 15 (2003) 218–220.
[15] A.L. Pyayt, Guiding light in electro-optic polymers, Polymers 3 (2011) 1591–1599.
[16] J.P. Drummond, S.J. Clarson, S. John, F. Zetts, K. Hopkins, S.J. Caracci, Enhanced electro-optic poling in guest–host systems using conductive polymer-based cladding layers, Applied Physics Letters 74 (1999) 368–370.
[17] M.D. Watson, P.R. Ashley, M. Abushagur, Modeling of optical waveguide poling and thermally stimulated discharge (TSD) charge and current densities for guest/host electro-optic polymers, IEEE Journal of Quantum Electronics 40 (2004) 1555–1561.
[18] Y.V. Pereverzev, O.V. Prezhdo, L.R. Dalton, Macroscopic order and electro-optic response of dipolar chromophore–polymer materials, Chemical Physics and Physical Chemistry 5 (2004) 1821–1830.
[19] C.M. Chen, F. Zhang, H. Wang, X.Q. Sun, F. Wang, Z.C. Cui, D.M. Zhang, UV curable electro-optic polymer switch based on direct photo definition technique, IEEE Journal of Quantum Electronics 47 (2011) 959–964.
[20] H.L. Rommel, B.H. Robinson, Orientation of electro-optic chromophores under poling conditions: a spheroidal model, Journal of Physical Chemistry C 111 (2007) 18765–18777.
[21] E.M. McKenna, A.S. Lin, A.R. Mickelson, D. Raluca, Jin, Dan, Comparison of γ_{33} values for AJ404 films prepared with parallel plate and corona poling, Journal of Optical Society of America B 24 (2007) 2888–2892.
[22] Y. Zhao, D.M. Zhang, F. Wang, Z.C. Cui, M.B. Yi, C.S. Ma, W.B. Guo, S.Y. Liu, Fabrication techniques for polymer/Si optical waveguide, Optics & Laser Technology 36 (2004) 657–660.
[23] X.Q. Sun, X.D. Li, C.M. Chen, K. Zhang, J. Meng, X.B. Wang, T.F. Yang, D.M. Zhang, F. Wang, Z.Y. Xie, Optimized inductively coupled plasma etching for poly(methyl-methacrylate-glycidly-methacrylate) optical waveguide, Thin Solid Films 520 (2012) 5946–5951.
[24] X. Wang, J. Meng, X. Sun, T. Yang, J. Sun, C. Chen, C. Zheng, D. Zhang, Inductively coupled plasma etching to fabricate sensing window for polymer waveguide biosensor application, Applied Surface Science 259 (2012) 105–109.
[25] M. Zenkiewicz, The applications of atom force microscopy in polymer studies, Polimery 44 (1999) 571–578.
[26] F. Walther, W.M. Heckl, R.W. Stark, Evaluation of nanoscale roughness measurements on a plasma treated SU-8 polymer surface by atomic force microscopy, Applied Surface Science 254 (2008) 7290–7295.
[27] Y.J. Cho, J.-S. Lee, J.-Y. Lee, Synthesis of novel Y-type nonlinear optical polyester with enhanced thermal stability of second harmonic generation for electro-optic applications, Bulletin of the Korean Chemical Society 31 (2010) 1509–1514.
[28] X.L. Zhang, M. Li, Z.S. Shi, Y. Wan, L.S.H. Zhao, R.L. Jin, X.B. Wang, D.M. Zhang, M.B. Yi, Z.C.H. Cui, Design, synthesis, and characterization of crosslinkable doped NLO materials based on polyurethanes containing spindle-type chromophores, Macromolecular Chemistry and Physics 212 (2011) 879–886.
[29] D. Bosc, A. Maalouf, S. Haesaert, F. Henrio, Investigation into defects occurring on the polymer surface during the photolithography process, Applied Surface Science 253 (2007) 6162–6164.
[30] C.C. Teng, H.T. Man, Simple reflection technique for measuring the electro-optic coefficient of poled polymers, Applied Physics Letters 56 (1990) 1734.
[31] C.T. DeRose, Ph.D. Dissertation, University of AZ College of Optical Science, 2009.
[32] S. Michel, J. Zyss, I. Ledoux-Rak, C.T. Nguyen, High-performance electro-optic modulators realized with a commercial side-chain DR1–PMMA electro-optic copolymer, Proceedings of SPIE 7599 (2010) 759901.
[33] J.G. Grote, J.S. Zetts, R.L. Nelson, F.K. Hopkins, C.H. Zhang, L.R. Dalton, W.H. Steier, Conductive cladding layers for electrode-poled nonlinear optic polymer electro-optics, Proceedings of SPIE 4114 (2000) 101.
[34] Q.S.H. Shen, K.Y. Wong, Improved thermal stability of poled polymers by optimized physical aging process, Optics Communications 164 (1999) 47–50.
[35] B.F. Yun, G.H. Hu, Ch.G. Lu, Y.P. Cui, Study on dipolar orientation and relaxation characteristics of guest–host polymers affected by corona poling parameters, Optics Communications 282 (2009) 1793–1797.
[36] D.H. Park, C.H. Lee, W.N. Herman, Analysis of multiple reflection effects in reflective measurements of electro-optic coefficients of poled polymers in multilayer structures, Optics Express 14 (2006) 8866–8884.
[37] S.J. Benight, D.H. Bale, B.C. Olbricht, L.R. Dalton, Organic electro-optics: understanding material structure/function relationships and device fabrication issues, Journal of Materials Chemistry 19 (2009) 7466–7475.
[38] F. Wan, G.O. Carlisle, K. Koch, D.R. Martinez, Enhanced second-harmonic response and stability of corona-poled guest–host polycarbonate thin films, Journal of Materials Science: Materials in Electronics 6 (1995) 228–234.
[39] M.J. Banach, M.D. Alexander Jr., S. Caracci, R.A. Vaia, Enhancement of electrooptic coefficient of doped films through optimization of chromophore environment, Chemistry of Materials 11 (1999) 2554–2561.
[40] H. Hayashi, H. Nakayama, O. Sugihara, N. Okamoto, Thermally stable and large second-order nonlinearity in poled silica films doped with Disperse Red 1 in high concentration, Optics Letters 20 (1995) 2264–2266.
[41] W. Shi, C.H.S.H. Fang, Q.W. Pan, Z.H.H. Qin, Q.T. Gu, D. Xu, J.Z.H. Yu, Optimization and characterization of the guest–host polyetherketone polymer films for application in integrated optical devices, Journal of Physics D: Applied Physics 35 (2002) 1404.
[42] B. Yang, L. Yang, R. Hu, Z. Sheng, D. Dai, Q. Liu, S. He, Fabrication and characterization of small optical ridge waveguides based on SU-8 polymer, Journal of Lightwave Technology 27 (2009) 4091–4096.
[43] H.-M. Lee, M.-C. Oh, H. Park, W.-Y. Hwang, J.-J. Kim, End-face scattering loss in integrated-optical waveguides, Applied Optics 36 (1997) 9021–9024.